



## Probing the nature of particle–core couplings in $^{49}\text{Ca}$ with $\gamma$ spectroscopy and heavy-ion transfer reactions

D. Montanari<sup>a,b,1</sup>, S. Leoni<sup>a,b,\*</sup>, D. Mengoni<sup>c,d</sup>, G. Benzoni<sup>b</sup>, N. Blasi<sup>b</sup>, G. Bocchi<sup>a</sup>, P.F. Bortignon<sup>a,b</sup>, A. Bracco<sup>a,b</sup>, F. Camera<sup>a,b</sup>, G. Colò<sup>a,b</sup>, A. Corsi<sup>a,b</sup>, F.C.L. Crespi<sup>a,b</sup>, B. Million<sup>b</sup>, R. Nicolini<sup>a,b</sup>, O. Wieland<sup>b</sup>, J.J. Valiente-Dobon<sup>e</sup>, L. Corradi<sup>e</sup>, G. de Angelis<sup>e</sup>, F. Della Vedova<sup>e</sup>, E. Fioretto<sup>e</sup>, A. Gadea<sup>f</sup>, D.R. Napoli<sup>e</sup>, R. Orlandi<sup>e,2</sup>, F. Recchia<sup>c,g</sup>, E. Sahin<sup>e</sup>, R. Silvestri<sup>e</sup>, A.M. Stefanini<sup>e</sup>, R.P. Singh<sup>e</sup>, S. Szilner<sup>h</sup>, D. Bazzacco<sup>g</sup>, E. Farnea<sup>g</sup>, R. Menegazzo<sup>g</sup>, A. Gottardo<sup>c,e</sup>, S.M. Lenzi<sup>c,g</sup>, S. Lunardi<sup>c,g</sup>, G. Montagnoli<sup>c,g</sup>, F. Scarlassara<sup>c,g</sup>, C. Ur<sup>g</sup>, G. Lo Bianco<sup>i</sup>, A. Zucchiatti<sup>j</sup>, M. Kmiecik<sup>k</sup>, A. Maj<sup>k</sup>, W. Meczynski<sup>k</sup>, A. Dewald<sup>l</sup>, Th. Pissulla<sup>l</sup>, G. Pollarolo<sup>m</sup>

<sup>a</sup> Dipartimento di Fisica, University of Milano, Milano, Italy

<sup>b</sup> INFN, Sezione di Milano, Milano, Italy

<sup>c</sup> Dipartimento di Fisica, University of Padova, Padova, Italy

<sup>d</sup> University of the West of Scotland, Paisley, UK

<sup>e</sup> INFN, Laboratori Nazionali di Legnaro, Padova, Italy

<sup>f</sup> IFIC CSIC – Universitat de València, Spain

<sup>g</sup> INFN, Sezione di Padova, Padova, Italy

<sup>h</sup> Ruder Bošković Institute, Zagreb, Croatia

<sup>i</sup> University of Camerino and INFN, Sezione di Perugia, Italy

<sup>j</sup> INFN Sezione di Genova, Genova, Italy

<sup>k</sup> The Niewodniczanski Institute of Nuclear Physics, Polish Academy of Sciences, Krakow, Poland

<sup>l</sup> Institut für Kernphysik der Universität zu Köln, Köln, Germany

<sup>m</sup> Dipartimento di Fisica Teorica, University of Torino and INFN, Sezione di Torino, Italy

### ARTICLE INFO

#### Article history:

Received 12 October 2010

Received in revised form 28 December 2010

Accepted 22 January 2011

Available online 27 January 2011

Editor: V. Metag

#### Keywords:

Multi-nucleon transfer

Gamma spectroscopy

Magnetic spectrometer

Particle–core coupling

### ABSTRACT

Neutron rich nuclei around  $^{48}\text{Ca}$  have been measured with the CLARA–PRISMA setup, making use of  $^{48}\text{Ca}$  on  $^{64}\text{Ni}$  binary reactions, at 5.9 MeV/A. Angular distributions of  $\gamma$  rays give evidence, in several transfer channels, for a large spin alignment ( $\approx 70\%$ ) perpendicular to the reaction plane, making it possible to firmly establish spin and parities of the excited states. In the case of  $^{49}\text{Ca}$ , states arising from different types of particle–core couplings are, for the first time, unambiguously identified on basis of angular distribution, polarization and lifetime measurements. Shell model and particle–vibration coupling calculations are used to pin down the nature of the states. Evidence is found for the presence, in the same excitation energy region, of two types of coupled states, i.e. single particle coupled to either  $^{48}\text{Ca}$  or  $^{50}\text{Ca}$  simple configurations, and particle–vibration coupled states based on the  $3^-$  phonon of  $^{48}\text{Ca}$ .

© 2011 Elsevier B.V. All rights reserved.

The understanding of particle–phonon and phonon–phonon couplings is at the basis of fermionic many-body interacting systems, both in solid state and nuclear physics. In particular, the coupling of a single particle to the vibrational motion is the key process at the origin of anharmonicities of the vibrational spectra and a building block of phonon–phonon interactions. In nuclear

physics, these couplings give rise to many important phenomena, such as the damping of collective excitations (as giant resonances), effective masses and spectroscopic factors [1–3]. Moreover, excitations of phonons and single-particle degrees of freedom play a role in reaction mechanisms between heavy ions, being responsible for the exchange of mass and charge in the reaction process [4].

Experimentally, several indications have been found of discrete states of particle–phonon nature (mostly in medium-heavy nuclei) [1,5–11], but only in few cases a clear evidence has been obtained. Therefore, it is still an open question whether states of particle–phonon nature can be considered a general nuclear prop-

\* Corresponding author at: University of Milano, Milano, Italy.

E-mail address: silvia.leoni@mi.infn.it (S. Leoni).

<sup>1</sup> Present address: University of Padova, Padova, Italy.

<sup>2</sup> Present address: IEM-CSIC, Madrid, Spain.

erty, also in rather light systems with reduced collectivity. In this context, the doubly magic nucleus  $^{48}\text{Ca}$  is particularly interesting, since candidates for multiple phonon states have been found, based on the coupling of the  $2^+$  and  $3^-$  [12]. However, while the  $2^+$  state has a very limited collectivity, the  $3^-$  has a rather strong collective character [12,13]. Therefore, it is interesting to verify if these properties manifest themselves also in adjacent nuclei, such as  $^{49}\text{Ca}$ , where states have been attributed to the coupling of core excitations with a single particle, either starting from  $^{48}\text{Ca}$  or  $^{50}\text{Ca}$  [14].

Structural information on  $^{49}\text{Ca}$  has been rather scarce and mainly limited, for long time, to particle spectroscopy [15–17]. This is generally true for all neutron-rich systems (even at the edge of the stability valley), which cannot be reached by standard fusion-evaporation reactions. A breakthrough in this field came in the last decade, when modern  $\gamma$  arrays made feasible in-beam  $\gamma$  spectroscopy with low-energy binary reactions in the grazing regime [18]. This has paved the way to even more selective studies with this type of reactions, which at present are largely profiting from the combined use of efficient  $\gamma$  arrays and large acceptance magnetic spectrometers [19,20].

In this Letter we present a complete in-beam  $\gamma$ -spectroscopy study of  $^{49}\text{Ca}$  states which are relevant in terms of couplings with core excitations. The levels of  $^{49}\text{Ca}$  are populated by the  $^{48}\text{Ca} + ^{64}\text{Ni}$  binary reaction, at energies approximately twice the Coulomb barrier. For the first time with heavy-ion transfer reactions, we clearly show the possibility of using angular distributions and polarization of the  $\gamma$  transitions to firmly establish spin and parity of the nuclear states. This is made possible by a large spin alignment (of the order of 70%), perpendicular to the reaction plane, significantly larger than typically observed in heavy ion transfer reactions at the Coulomb barrier [21,22] and also in deep-inelastic heavy ion collisions at intermediate and relativistic energy [23,24]. Moreover, we fully establish the microscopic nature of these states by comparing the experimental  $B(E\lambda)$  values (extracted from lifetime measurements) with predictions based on shell model and particle-vibration coupling calculations. The work clearly demonstrates the feasibility of complete in-beam  $\gamma$  spectroscopy with heavy-ion transfer reactions, providing a method that can be exploited also in the future with heavy targets and radioactive beams.

The experiment was performed at Laboratori Nazionali di Legnaro (LNL) of INFN (Italy) [25]. The  $^{48}\text{Ca}$  beam, impinging on a  $0.98 \text{ mg/cm}^2$  thick  $^{64}\text{Ni}$  target, was provided by the Tandem-Alpi accelerators at 282 MeV, with an average current of 1 pA. The reaction populated several multi-nucleon transfer channels, with average  $v/c$  velocity of  $\sim 10\%$  and 2% for projectile- and target-like nuclei, respectively. The reaction products were measured by the large acceptance ( $\sim 80 \text{ msr}$ ) magnetic spectrometer PRISMA [26] and the coincident  $\gamma$  rays by the CLARA HPGe array [19]. In the experiment PRISMA was placed at the grazing angle for this reaction, i.e.  $20^\circ$ , with an angular acceptance of  $\pm 6^\circ$ . The Ge array CLARA consisted of 23 composite Ge detector of EUROBALL Clover type [27], each equipped with anti-Compton shields, for a total absolute efficiency of  $\sim 3\%$  at 1.3 MeV. The Clover detectors were arranged in a hemisphere opposite to PRISMA with the Ge crystals placed in three rings at average azimuthal angles  $\theta_{CLA} = 100^\circ, 130^\circ$  and  $150^\circ$  with respect to the entrance direction of the spectrometer. In this way reaction products detected in the spectrometer focal plane have a forward trajectory with respect to the Ge array. The Doppler correction of the  $\gamma$  rays emitted by the projectile-like nuclei was performed on event-by-event basis using the velocity and angle provided by the trajectory reconstruction in PRISMA [28]. This resulted in an energy resolution of  $\sim 5 \text{ keV}$  at 600 keV and  $\sim 34 \text{ keV}$  at 3.8 MeV (i.e. consistent with the uncertainty associated to the opening angle of the Ge crystals).

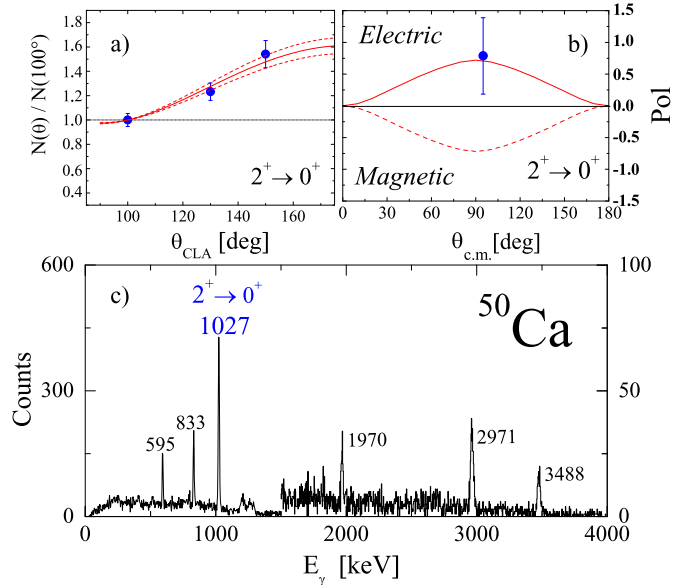


**Fig. 1.** Bottom panel: Gamma spectrum (with 3 keV/ch) measured in coincidence with  $^{50}\text{Ca}$  ions detected in PRISMA. Note that above 1500 keV the scale of the y axis is given on the right. Panel (a): Angular distribution of the  $2^+ \rightarrow 0^+$  transition at 1027 keV. The solid line is the fit by the angular distribution function  $W(\theta) = 1 + a_2 P_2(\cos\theta)$ , with  $a_2 = 0.51 \pm 0.06$ . The dotted lines give the uncertainty in  $W(\theta)$ , as follows from the error propagation in the  $a_2$  coefficient. Panel (b): Polarization measurement of the  $2^+ \rightarrow 0^+$  transition. Solid and dashed lines give the expected values for a pure electric or magnetic quadrupole decay.

Due to the limited efficiency of the CLARA array, extended analysis of the  $\gamma$  spectra could only be performed for reaction products with higher cross sections. No  $\gamma$ - $\gamma$  correlations could be made, being however the level scheme well established by previous works with higher efficiency arrays [18]. In the present work the angular distributions of the strongest  $\gamma$  transitions have been studied, grouping the Ge detectors in the three rings. The validity of the analysis is demonstrated in Fig. 1 in the  $^{50}\text{Ca}$  case. The bottom panel shows the  $\gamma$  spectrum detected in coincidence with  $^{50}\text{Ca}$  ions in PRISMA. All strong peaks are transitions with a tentative spin and parity assignments, the only firm case being the  $2^+ \rightarrow 0^+$  decay of 1027 keV [18]. The angular distribution analysis of this very intense and clean transition is shown in panel (a). The intensities measured in the three rings have been normalized to the one at  $100^\circ$ , after a careful evaluation of the efficiency of each ring. The data have been fitted using the angular distribution function  $W(\theta) = 1 + a_2 P_2(\cos\theta)$ , being  $P_2(\cos\theta)$  the Legendre polynomial and  $a_2$  the fitting parameter. Because of the high  $v/c$  of the projectile-like products, we have also taken into account the relativistic correction to the angular distribution [23]. The  $a_2$  coefficient can be precisely calculated for a given  $\gamma$  decay with fully aligned nuclear spin [29,30], providing a maximum value,  $a_{2\max}$ , which can be compared with the experiment. It is found that  $a_{2\max}$  is given by the product  $A_2 B_2$ , being  $A_2$  the angular distribution coefficient (depending on the multipolarity of the transition) and  $B_2$  the orientation parameter (depending on the orientation mechanism and the spin of the nuclear state). The anisotropy observed in  $W(\theta)$  for the  $2^+ \rightarrow 0^+$  transition of  $^{50}\text{Ca}$  is consistent with a stretched quadrupole transition with spin aligned perpendicularly to the reaction plane. We find  $a_2 = 0.51 \pm 0.06$ , which correspond to a large fraction of spin alignment  $\alpha_2 = a_2/a_{2\max} = 0.71 \pm 0.08$ . A measurement of the linear polarization  $P$  has also been performed, making use of the most sensitive Clover detectors at  $100^\circ$ .  $P$  is defined as the ratio  $A_{\text{sym}}/Q$ , with  $A_{\text{sym}} = (N_\perp - N_\parallel)/(N_\perp + N_\parallel)$  the measured asym-

metry in the number of photon scattered perpendicular ( $N_{\perp}$ ) and parallel ( $N_{\parallel}$ ) in the Clover crystals.  $Q$  is the polarimeter sensitivity (depending on the energy of the  $\gamma$  ray), which is experimentally determined from known transitions. Fig. 1(b) shows the polarization analysis of the 1027-keV transition, clearly indicating the electric character of the  $\gamma$ -decay. Similar results are obtained for a number of known stretched electric quadrupole transitions belonging to  $^{46,48,50}\text{Ca}$  and  $^{51}\text{Sc}$  nuclei. This is shown in Fig. 2, where we give the measured fraction  $\alpha_2$  of full alignment, resulting in an average value of the order of 70%. Therefore, it is clear that a large spin alignment is a common feature of these grazing collisions, involving the exchange of few nucleons.

The techniques described above have been used to establish spin and parity of the excited states of  $^{49}\text{Ca}$  up to  $\sim 4$  MeV of excitation energy (see right part of Fig. 3). In this energy region,  $^{48}\text{Ca}(\text{d}, \text{p})^{49}\text{Ca}$  transfer reactions provided spectroscopic informa-

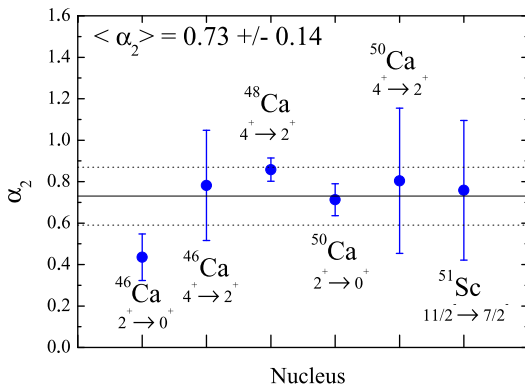


**Fig. 2.** Fraction  $\alpha_2$  of full spin alignment obtained from the experimental angular distributions of known stretched E2 transitions, following the decay of  $^{46,48,50}\text{Ca}$  and  $^{51}\text{Sc}$  nuclei, populated in the  $^{48}\text{Ca} + ^{64}\text{Ni}$  reaction. The average value  $\alpha_2 = 0.73 \pm 0.14$  is indicated by lines.

tion on a number of excited states using the Distorted-Wave-Born approximation approach [15–17]. In particular, the ground state of  $^{49}\text{Ca}$  was found to be a single particle  $p_{3/2}$  neutron state, while the states at 2.022 and 3.991 MeV were identified as  $p_{1/2}$  and  $f_{5/2}$  single particle neutron states, with spectroscopic factors  $\sim 0.8\text{--}0.9$ . Three additional states were also observed, at energy close to 3.357, 3.589 and 4.017 MeV, all showing a reduced fraction of single particle component (i.e. spectroscopic factors  $\leq 0.3$ ). While the 3.589- and 4.017-MeV states were interpreted as  $J^\pi = 5/2^-$  and  $9/2^+$  state (with large uncertainty due to the limited energy resolution of the detected particles), the state at 3.357 MeV showed a very anomalous angular distribution of the scattered proton, leading to a questionable assignment ( $J^\pi = 9/2^+$ ). These states were never unambiguously identified even in more recent  $\gamma$ -spectroscopy studies [18] (e.g. by measuring the character and multipolarity of the transitions involved). Therefore, a tentative spin and parity assignment has been adopted, so far, mostly based on systematics and comparison with model predictions, leaving open, in particular, the interesting issue of the nature of particle-core coupled states.

As schematically illustrated in Fig. 3, a particle–core coupling scheme has been proposed to explain the nature of the “anomalous”  $^{49}\text{Ca}$  states at excitation energies in the region of the first excited states of  $^{48}\text{Ca}$  [14], although without a complete theoretical interpretation. In particular, the coupling of the  $3^-$  phonon of  $^{48}\text{Ca}$  with the unpaired  $p_{3/2}$  neutron of  $^{49}\text{Ca}$  is expected to give rise to a multiplet of states with  $J^\pi = 9/2^+, 7/2^+, 5/2^+$  and  $3/2^+$ , while shell model calculations provide the negative parity states in terms of simple single-particle or two particles-one hole (2p-1h) configurations, based either on  $^{48}\text{Ca}$ - or  $^{50}\text{Ca}$ -core states.

Fig. 4 shows the  $\gamma$  spectrum measured in the CLARA array in coincidence with  $^{49}\text{Ca}$  ions detected in PRISMA. All strong transitions correspond to the decays from the states discussed above and reported in the right panel of Fig. 3. Although the energy res-

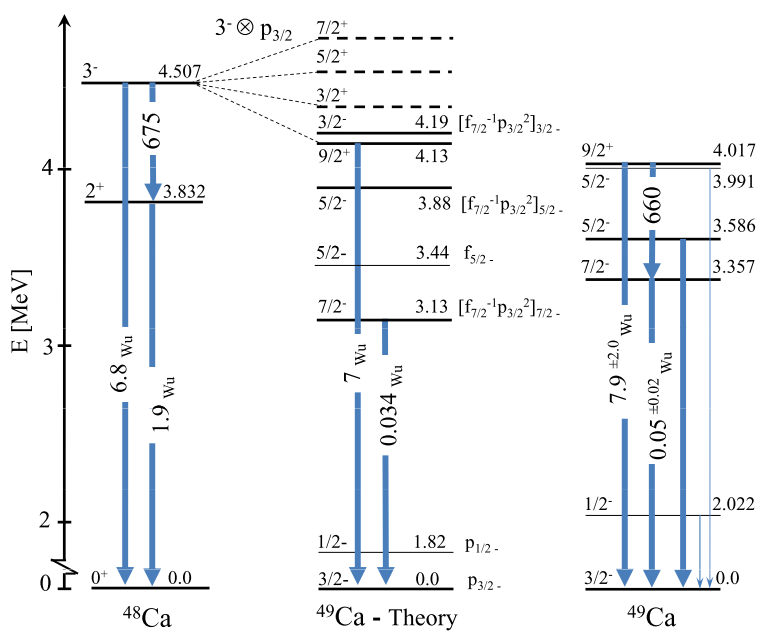


**Fig. 3.** Right: decay scheme of  $^{49}\text{Ca}$  as observed in this work, with level energies (right labels) taken from Refs. [14,18]. Thin arrows indicate the  $\gamma$  decay from states of single particle nature (also indicated by thin lines). Center: calculated levels of  $^{49}\text{Ca}$ . Positive parity states are obtained with the particle-vibration coupling method [1], negative parity states by the full fp shell model of Ref. [31], with dominant configurations given on the right side of each level. We note that 2p-1h states with  $[f_{7/2}^{-1}p_{3/2}^2]$  character can in principle be generated either by coupling a  $p_{3/2}$  particle with the  $2^+$  state of  $^{48}\text{Ca}$  (with dominant configuration  $[f_{7/2}^{-1}p_{3/2}]_{2+}$ ) or by coupling a  $f_{7/2}^{-1}$  hole to the  $0^+$  or  $2^+$  states of  $^{50}\text{Ca}$ , with dominant configuration  $[p_{3/2}^2]_{0+}$  and  $[p_{3/2}^2]_{2+}$ , respectively (see, however, the discussion in the text). On the left, the experimental  $2^+$  and  $3^-$  levels of  $^{48}\text{Ca}$  are given [32]. The  $B(E\lambda)$  strengths of the relevant  $\gamma$  transitions are reported on the arrows in Weisskopf units (Wu) (from Refs. [12,13] and present work).

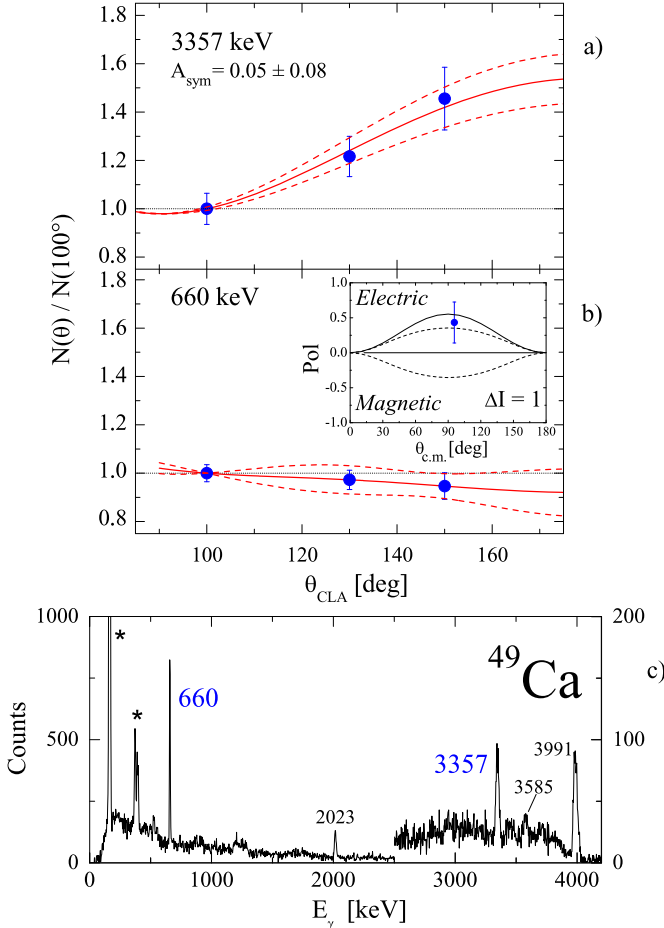


**Fig. 4.** Bottom panel: Gamma spectrum (with 3 keV/ch) measured in coincidence with  $^{49}\text{Ca}$  ions detected in PRISMA. Contaminant lines from  $^{63}\text{Ni}$  are marked by stars. Note that above 2500 keV the scale of the y axis is given on the right. Panels (a) and (b): Angular distribution of the 3357- and 660-keV transitions. The solid lines are the fit by the function  $W(\theta)$ , with parameters  $a_2 = 0.47 \pm 0.07$  and  $0.072 \pm 0.05$ , respectively. The dotted lines give the uncertainty in  $W(\theta)$  following the error propagation in  $a_2$ . The inset of panel (b) gives the polarization of the 660-keV  $\gamma$  ray in comparison with prediction for a pure electric or magnetic dipole (dashed lines). The solid line gives the expected values for an electric dipole with a 4% quadrupole component. For the 3357-keV transition only the asymmetry value  $A_{\text{sym}} = 0.05 \pm 0.08$  is given, which support the electric nature of the  $\gamma$  decay.

olution of this experiment is up to four times larger than in the stopped recoil (thick target) measurements of Ref. [18], the centroid values agree within 3 keV. In particular, the  $\gamma$  transition of 3357 keV has been proposed by Broda et al. [18] as the ground-state decay from the  $7/2^-$  level (tentatively assigned to  $(9/2^+)$ ) by particle spectroscopy studies [16,17], which should correspond to a pure 2p-1h configuration either arising from the coupling of the  $2^+$  of  $^{48}\text{Ca}$  with the  $p_{3/2}$  neutron or from a  $f_{7/2}^{-1}$ -neutron hole coupled to the ground state of  $^{50}\text{Ca}$ . The 660 keV line is instead suggested as the decay from the  $9/2^+$  state, which is the lowest member of the particle-vibration coupling multiplet with the  $3^-$  state of  $^{48}\text{Ca}$  (see Fig. 3). A very weak 3585-keV transition is also observed, which should be the ground-state decay from the  $5/2^-$  state of 2p-1h nature, while the direct 4017-keV  $9/2^+ \rightarrow 3/2^-$  transition falls in the tail of the strong 3991-keV line, deexciting the single-particle  $5/2^-$  level [14]. The angular distributions of the 3357- and 660-keV transitions are shown in Fig. 4(a) and (b). They are fitted by the  $W(\theta)$  functions with parameters  $a_2 = 0.47 \pm 0.07$  and  $0.072 \pm 0.05$ , respectively, which are consistent with stretched quadrupole and dipole transitions, with a

small component of quadrupole decay ( $\sim 4\%$ ) for the 660-keV line. In addition, polarization measurements performed with the  $100^\circ$  detectors indicate an electric character for both transitions (see Fig. 4), therefore fixing the spin and parity of these states to  $7/2^-$  and  $9/2^+$ . It is worth noticing that the present  $7/2^-$  assignment is also consistent with the neutron knockout reaction study at relativistic energies of Ref. [33], which observes an  $l = 3$  component in the momentum distribution of the  $^{49}\text{Ca}$  fragment in coincidence with the 3357-keV  $\gamma$  line.

To investigate the microscopic nature of the  $7/2^-$  and  $9/2^+$  states and fully establish the core-coupling scheme, lifetime analysis has been performed, using the differential recoil distance Doppler shift method on the same data set which has been successfully used in the case of  $^{50}\text{Ca}$  and  $^{51}\text{Sc}$  [34,35]. Fig. 5 shows, for different target-to-degrader distances, Doppler-corrected  $\gamma$ -ray spectra of  $^{49}\text{Ca}$  in the energy regions including the  $9/2^+ \rightarrow 7/2^-$  660-keV line (panels (c), (e), (g)) and the  $7/2^- \rightarrow 3/2^-$  3357-keV transition (panels (d), (f) and (h)). The spectra show, for each transition, two peaks, depending on whether the  $\gamma$  ray was emitted before or after the degrader. The lifetimes of the state of interest (top panels (a) and (b)) are determined by the relative intensities  $R = \frac{I_{\text{After}}}{I_{660}}$ , as a function of the target-to-degrader distances, being  $I_{\text{After}}$  the peak area after the degrader and  $I_{660}$  the total intensity of the 660-keV line. The lifetime obtained for the  $9/2^+$  and  $7/2^-$  states are  $\tau = 8.5 \pm 2.0$  ps and  $3.5 \pm 1.4$  ps, respectively. In the latter case, the feeding contribution from the 660-keV transition to the  $7/2^-$  state has been taken into account by a two steps decay model [36]. While the  $7/2^-$  state has 100% branching to the  $3/2^-$  ground state, in the  $9/2^+$  case the direct branching to the ground state is 9.2% [18], which gives a partial lifetime of  $92 \pm 23$  ps for the E3 transition of 4017 keV. From these experimental lifetime we obtain  $B(E2) = 0.05 \pm 0.02$  Wu for the 3357-keV transition and  $B(E3) = 7.9 \pm 2.0$  Wu for the 4017-keV line, the latter being close to the  $B(E3)$  value of the  $3^-$  state of  $^{48}\text{Ca}$ .

The interpretation of the observed  $B(E\lambda)$  values and of the nature of the states in  $^{49}\text{Ca}$  has been based on the two different theoretical approaches presented in Fig. 3. In fact, the  $3^-$  state at 4.507 MeV in  $^{48}\text{Ca}$  exhibits a sizable collectivity, with a measured  $B(E3)$  of 6.8 Wu [13]. By performing microscopic Skyrme-RPA calculations [37], employing the parameter set SLy5 [38], we are able to well reproduce the energy and the  $B(E3)$  of the  $3^-$  state in  $^{48}\text{Ca}$ . Although a small number of p-h configurations is found to significantly contribute, the corresponding proton and neutron transition densities are consistent with a shape vibration, therefore supporting the collective character of the  $3^-$  state. On the other hand, the  $2^+$  state of  $^{48}\text{Ca}$  has been described as a non collective 1p-1h configuration with a dominating  $[f_{7/2}^{-1}, p_{3/2}]_{2+}$  component [39]. This interpretation is consistent with the rather small  $B(E2)$  value ( $\approx 1.9$  Wu) experimentally measured [12]. Therefore, we describe the  $9/2^+$  state of  $^{49}\text{Ca}$  by applying a particle-vibration weak coupling scheme [1], while we make use of shell model calculations to interpret the nature of the  $7/2^-$  state.

The shell model calculations have been performed by the code ANTOINE [41,42] in the full  $fp$  shell and with the KB3G effective interaction [31]. For the calculation of the transition probabilities standard values of the effective charges for the  $fp$  shell have been used ( $e_\pi = 1.5e$ ,  $e_\nu = 0.5e$ ), as established by the lifetime measurement of Ref. [34]. The calculations reproduce rather well both the excitation energy and the E2 strength of the  $7/2^-$  state, being  $E = 3.134$  keV and  $B(E2) = 0.034$  Wu, with a dominant configuration ( $\sim 80\%$ ) of  $[f_{7/2}^{-1} p_{3/2}^2]$  type. Moreover, the rather different  $B(E2)$  values measured for the  $7/2^-$  state of  $^{49}\text{Ca}$  and the  $2^+$  state of  $^{48}\text{Ca}$  cannot lead us to interpret the  $7/2^-$  state in terms of a  $p_{3/2}$  neutron coupled to the  $2^+$  state of  $^{48}\text{Ca}$  [40]. Our interpre-

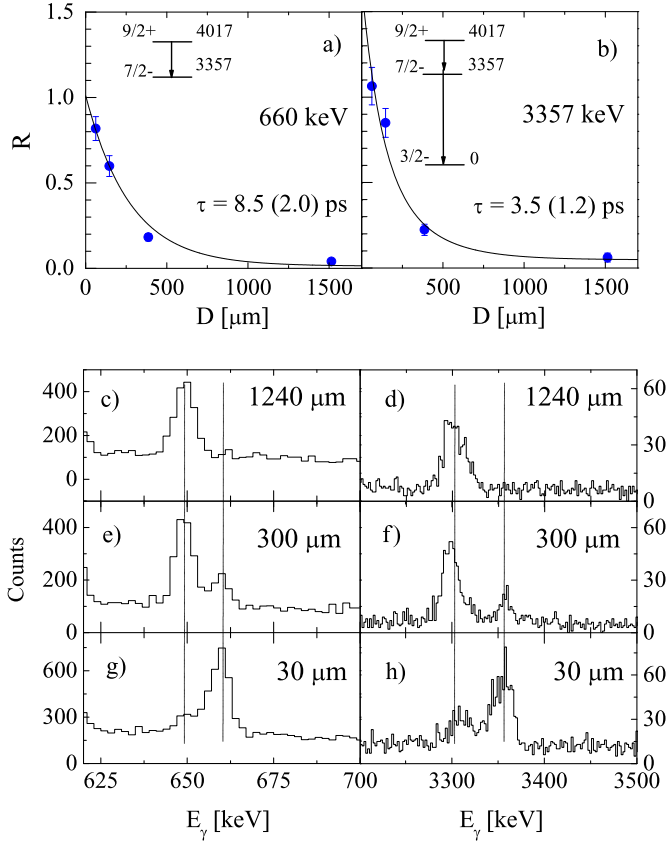


**Fig. 5.** Bottom panels: Doppler corrected  $\gamma$ -ray spectra showing the 660-keV ((c), (e) and (g)) and 3357-keV ((d), (f) and (h)) transitions of  $^{49}\text{Ca}$ . The higher-energy and lower-energy peaks correspond to the decays after and before the degrader, respectively, for the target-to-degrader distances  $D = 30, 300$  and  $1240 \mu\text{m}$ . The top panels (a) and (b) give the corresponding experimental ratio  $R = I_{\text{After}}/I_{660}$ , as a function of the effective target-to-degrader distances.

tation is more in favor of a 2p-1h state produced by coupling a  $f_{7/2}^{-1}$ -neutron hole to the  $0^+$  core of  $^{50}\text{Ca}$  (which is dominated by the paired  $[p_{3/2}]_{0+}$  neutrons). We note that a  $7/2^-$  state, with energy around 3.1 MeV and largely dominated by a  $[f_{7/2}^{-1}p_{3/2}^2]$  component, is also obtained by different shell model calculations, as reported in Refs. [39,43].

In the case of the  $3^- \otimes p_{3/2}$  multiplet, we have applied the weak coupling particle-vibration model of Bohr and Mottelson. The energies of the multiplet are shifted with respect to the unperturbed particle plus phonon energy by the amount associated with the diagrams (a)–(d) of Figs. 6–10 of Ref. [1]. We have calculated these shifts phenomenologically, by using the experimental energy and  $B(E3)$  value of the  $3^-$  phonon. The values of the single-particle energies are not all known, but we have used the Hartree-Fock results obtained with the effective force SkX [44], since this has been fitted using the known energies. In this way, the result for the energy of the  $9/2^+$  level is in good agreement with the finding of our experiment (see Fig. 3). It has to be noted that the energy of the levels arising from the coupling of the  $3^-$  with particle states lying in the continuum cannot be unambiguously determined (as indicated by the use of dashed lines in the figure). Moreover, at the lowest perturbative order, the  $B(E3)$  value associated with the decay of the member of the multiplet should be equal to the one associated with the phonon de-excitation. This is also experimentally confirmed, so that we can conclude there is strong evidence that the  $9/2^+$  state at 4017 keV in  $^{49}\text{Ca}$  has a particle-phonon nature.

In summary, the binary reaction  $^{48}\text{Ca} + ^{64}\text{Ni}$ , at energies twice the Coulomb barrier, has been used to investigate the structure of neutron rich nuclei in the region around the doubly magic nucleus  $^{48}\text{Ca}$ , with the PRISMA-CLARA setup at LNL. Evidence is found for a large spin alignment perpendicular to the reaction plane, which makes possible to use angular distributions and polarizations of the  $\gamma$  transitions to firmly establish spin and parity of the excited states. This represents a step forward in  $\gamma$ -spectroscopy studies with heavy ions grazing reactions at low energies, since it opens up the possibility to investigate in great details the properties of moderately neutron rich systems moving away from stability. In the specific case of  $^{49}\text{Ca}$ , the spectroscopic information probes the nature of the first excited states, giving evidence for two different types of particle-core couplings, either based on particle-phonon interactions or characterized by 2p-1h simple configurations. In the latter case the measured  $B(E\lambda)$  values give also the possibility to disentangle between equivalent configurations based on different core states ( $^{48}\text{Ca}$  or  $^{50}\text{Ca}$ ). In particular, it has to be noted that the  $9/2^+$  state at 4017 keV in  $^{49}\text{Ca}$  represents one of the few fully established examples of particle-vibration coupling in nuclei with mass  $A < 100$ , showing the robustness of nuclear collectivity in rather light systems. The present work makes clearly visible the multifaceted nature of particle-core coupling interactions in the atomic nucleus, giving also a warning to simple generalizations of coupling schemes.

## Acknowledgements

The authors wish to thank E. Vigezzi for fruitful discussions. This work was supported by the Italian Istituto Nazionale di Fisica Nucleare and partially by the Spanish MICINN (ACI2009-1070 bilateral action) and Generalitat Valenciana (Grant Nos. BEST/2009/073 and PROMETEO/2010/101). The work has also been partially supported by the Polish Ministry of Science and Higher Education (Grant No. N N202 309135).

## References

- [1] A. Bohr, B.R. Mottelson, Nuclear Structure, vols. I and II, W.A. Benjamin, 1975.
- [2] P.F. Bortignon, A. Bracco, R.A. Broglia, Giant Resonances: Nuclear Structure at Finite Temperature, Harwood Academic Publishers, New York, 1998.
- [3] V.G. Soloviev, The Theory of Atomic Nuclei: Quasiparticles and Phonons, Institute of Physics Publishing, Bristol and Philadelphia, 1995.
- [4] A. Winther, Nucl. Phys. A 594 (1995) 203.
- [5] N. Pietralla, et al., Phys. Lett. B 681 (2009) 134.
- [6] P. Kleinheinz, Phys. Scr. 24 (1981) 236.
- [7] P. Kleinheinz, et al., Phys. Rev. Lett. 48 (1982) 1457.
- [8] S. Gales, Ch. Stoyanov, A.I. Vdovin, Phys. Rep. 166 (1988) 125.
- [9] C.J. Lister, et al., J. Phys. G: Nucl. Part. Phys. 6 (1980) 619.
- [10] A.M. Oros-Peusquens, P.F. Mantica, Nucl. Phys. A 669 (2000) 81.
- [11] T.P. Batsch, et al., Phys. Scr. 31 (1988) 843.
- [12] T. Hartmann, et al., Phys. Rev. C 65 (2002) 034301.
- [13] R.A. Einstein, et al., Phys. Rev. 188 (1969) 1815.
- [14] T.R. Canada, et al., Phys. Rev. C 4 (1971) 471.
- [15] W.D. Metz, W.D. Callender, C.K. Bockelman, Phys. Rev. C 12 (1975) 827.
- [16] R. Abegg, J.D. Hutton, M.E. Williams-Norton, Nucl. Phys. A 303 (1978) 121.
- [17] Y. Uozumi, et al., Nucl. Phys. A 576 (1994) 123.
- [18] R. Broda, J. Phys. G: Nucl. Part. Phys. 32 (2006) R151.
- [19] A. Gadea, et al., Eur. Phys. J. A 20 (2004) 193.
- [20] L. Corradi, G. Pollarolo, S. Szilner, J. Phys. G: Nucl. Part. Phys. 36 (2009) 113101.
- [21] T.C. Zhang, et al., Nucl. Phys. A 628 (1998) 386.
- [22] P. Aguer, et al., Phys. Rev. Lett. 43 (1979) 1778.
- [23] H. Olliver, T. Glasmacher, A.E. Stuchbery, Phys. Rev. C 68 (2003) 044312.
- [24] M. Kmiecik, et al., Eur. Phys. J. A 45 (2010) 153.
- [25] D. Montanari, et al., Acta Phys. Pol. B 40 (2009) 585.
- [26] A.M. Stefanini, et al., Nucl. Phys. A 701 (2002) 217c.
- [27] G. Duchene, et al., Nucl. Instrum. Methods A 432 (1999) 90.
- [28] D. Montanari, et al., Eur. Phys. J. A 47 (2011) 4.
- [29] A.H. Wapstra, et al., Nuclear Spectroscopy Tables, North-Holland, Amsterdam, 1959, VII.
- [30] T. Yamazaki, Nucl. Data A 3 (1967) 1.

- [31] A. Poves, et al., Nucl. Phys. A 694 (2001) 157.
- [32] R. Broda, Acta Phys. Pol. B 32 (2001) 2577.
- [33] R. Krücken, Am. Inst. Phys. Conf. Proc. 1972 (2008) 52.
- [34] J.J. Valiente-Dobon, et al., Phys. Rev. Lett. 102 (2009) 242502.
- [35] D. Mengoni, et al., Eur. Phys. J. A 42 (2009) 387.
- [36] D. Mengoni, et al., Phys. Rev. C 82 (2010) 024308.
- [37] G. Colò, et al., Nucl. Phys. A 788 (2007) 137c.
- [38] E. Chabanat, et al., Nucl. Phys. A 643 (1998) 441.
- [39] P. Federman, S. Pittel, Nucl. Phys. A 155 (1970) 161.
- [40] A. De-Shalit, Phys. Rev. 122 (1961) 1530.
- [41] E. Caurier, Shell-model code ANTOINE, IRES, Strasbourg, 1989.
- [42] E. Caurier, F. Nowacki, Acta Phys. Pol. 30 (1999) 705.
- [43] L. Coraggio, Phys. Rev. C 80 (2010) 044311.
- [44] B.A. Brown, Phys. Rev. C 58 (1998) 220.